Fluorite-Related Phases in the System Li-Pt-Sn: Synthesis and Structures of Li_2PtSn, $Li_3Pt_2Sn_3$, $Li_{2.27}Pt_2Sn_{3.73}$ and $Li_{2.43}Pt_2Sn_{3.57}$

Rolf-Dieter Hoffmann,[a] Zhiyun Wu,[a] and Rainer Pöttgen*[a]

In memory of Ron Snaith

Keywords: Lithium / Tin / Platinum / Intermetallic phases

The intermetallic compounds Li_2PtSn, $Li_3Pt_2Sn_3$, $Li_{2.27}Pt_2Sn_{3.73}$ and $Li_{2.43}Pt_2Sn_{3.57}$ were synthesised by reaction of the elements in sealed tantalum tubes. They were investigated by X-ray diffraction on powders and single crystals: $F\bar{4}3m$, a = 626.0(1) pm, $wR2$ = 0.0834, 70 F^2 values, 7 variables for Li_2PtSn; $Ia\bar{3}$, a = 1264.3(1) pm, $wR2$ = 0.0340, 416 F^2 values, 23 variables for $Li_3Pt_2Sn_3$; $Ia\bar{3}$, a = 1269.7(1) pm, $wR2$ = 0.1130, 521 F^2 values, 24 variables for $Li_{2.27(1)}Pt_2Sn_{3.73(1)}$; $Ia\bar{3}$, a = 1266.6(1) pm, $wR2$ = 0.1094, 620 F^2 values, 25 variables for $Li_{2.43(1)}Pt_2Sn_{3.57(1)}$. The latter refinement was based on a crystal twinned by merohedry. Li_2PtSn crystallises with an ordered variant of the BiF_3 type. The other stannides adopt a superstructure of the fluorite type where all three subcell axes are doubled. In $Li_3Pt_2Sn_3$ the platinum atoms are located on the calcium sites while the tin and 1/3 of the lithium atoms are ordered on the fluorine site. The remaining lithium atoms fill octahedral voids of the *fcc* arrangement of platinum. The superstructure is discussed on the basis of a group-subgroup scheme and experimental evidence is given for a solid solution $Li_{3-x}Pt_2Sn_{3+x}$.

Introduction

The binary fluoride BiF_3[1] has three crystallographic positions, Bi on the Wyckoff site 4*a*, F1 at 4*b*, and F2 at 8*c*. This structure type may be described as a filled fluorite variant with F1 in the octahedral voids or as a filled blende-type structure with half of the F2 atoms in the remaining tetrahedral voids and the F1 atoms in the octahedral voids. A variety of intermetallic lithium compounds adopt BiF_3-related structures. According to the different Wyckoff positions, the compositions Li_2TX, LiT_2X and $LiTX_2$ (T = late transition metal; X = *p*-block element of the 3rd or 4th group) are possible. Indeed, examples are known for all of them.[2] A large variety of such intermetallics were synthesised in the groups of Schuster[3,4] and Weiss[5] 30 years ago. Most of these intermetallics, however, have only been characterised on the basis of X-ray powder diffraction data.

Depending on the composition as well as on the T and X components, the compounds Li_2TX, LiT_2X and $LiTX_2$ have different electron counts, leading to a variety of interesting physical properties. Susceptibility and resistivity measurements reveal metallic behaviour and Pauli paramagnetism.[3,6] One of the most interesting properties of these intermetallics is the intrinsic colour,[3,6,7] which varies with the valence electron concentration. To give an example, in the solid solution $Li_{2-x}Mg_xPdSn$, the colour changes from brass yellow via copper red to red violet with increasing x.[7] The optical constants have been determined from reflection spectroscopic data.[3,6,7] At least some of the Li_2TX, LiT_2X and $LiTX_2$ compounds show lithium mobility.[8,9] Chemical bonding in various Li_2TX and $LiTX_2$ (T = Rh, Pd, Ir, Pt; X = Al, Ga, In) intermetallics has been investigated by X-ray photoelectron and X-ray excited Auger spectroscopy paralleled by DFT electronic structure calculations.[10,11]

In the course of our systematic studies on structure/property relation of Li-*T*-Sn stannides,[12–14] we have investigated the ternary system lithium-platinum-tin in more detail. It turned out that a large solid solution $Li_{3-x}Pt_2Sn_{3+x}$ (x = 0–1) exists with a fluorite subcell structure. $PtSn_2$ [15] crystallises with a fluorite structure and Li_2PtSn has a fluorite type subcell as well. In the superstructure with the ideal formula $Li_3Pt_2Sn_3$ the lithium and tin atoms are well ordered in a 2 × 2 × 2 cubic supercell. The process of lithium filling and Sn/Li substitution is formally done in two steps. At first the octahedral sites in $PtSn_2$ are filled to get "$LiPtSn_2$" and secondly tin is substituted by lithium on the tetrahedral sites up to Li_2PtSn.[16,17] The synthesis and crystal chemistry of these stannides is reported herein.

[a] Institut für Anorganische und Analytische Chemie and Sonderforschungsbereich 458, Universität Münster, Wilhelm-Klemm-Straße 8, 48149 Münster, Germany, E-mail: pottgen@uni-muenster.de

Results

A fluorite-type arrangement heavily governs the structural chemistry in the ternary system Li-Pt-Sn. The binary stannide $PtSn_2$ crystallises in the CaF_2 type. From the literature it is not known whether $PtSn_2$ has a noticeable range of homogeneity. This is also suggested by our own phase-analytical investigations within this work.

In the ternary compounds Li_2PtSn and $Li_3Pt_2Sn_3$ (better formulated as $Li_{3-x}Pt_2Sn_{3+x}$ with $x = 0-1$) the *ccp* arrangement of platinum atoms remains fixed, while lithium fills the octahedral voids and in addition substitutes tin atoms on the tetrahedral sites (Table 1 and 2, Figure 1). This filling is done in two steps. First, the octahedral sites are filled and then the Sn/Li substitution sets in. This conclusion can be drawn from Figure 2. For comparison reasons the lattice parameters of $PtSn_2$ and Li_2PtSn have been doubled to compare to the supercell of $Li_3Pt_2Sn_3$ (Table 3). Binary $PtSn_2$ has the largest lattice parameter, leading to a Sn−Sn distance of 321 pm which nicely matches the distance in elemental tin: 4×302 and 2×318 pm in β-Sn.[18] The Pt−Sn contacts are 278 pm comparing well to the sum of Pauling's single bond radii.[19] Incorporation of lithium at octahedral voids lets the lattice parameter sharply drop by about 16 pm resulting in shorter Pt−Sn distances (Table 4) than those in binary $PtSn_2$. The excess electrons from the lithium atoms, therefore, presumably fill bonding Pt−Sn states. The ideal structure $LiPtSn_2$, where only octahedral voids are filled by lithium, was not obtained. The extrapolated lattice parameter is indicated by an open circle in Figure 2. The composition with the lowest lithium content was $Li_{1.11}PtSn_{1.89}$ with 5.5% lithium on the tin site, whereas the highest lithium content in the superstructure was 25% corresponding to the ideal composition $Li_3Pt_2Sn_3$.

Table 1. Crystal data and structure refinement parameters for Li_2PtSn, $Li_3Pt_2Sn_3$, $Li_{2.43}Pt_2Sn_{3.57}$ and $Li_{2.27}Pt_2Sn_{3.73}$

Empirical formula	Li_2PtSn	$Li_3Pt_2Sn_3$	$Li_{2.43}Pt_2Sn_{3.57}$	$Li_{2.27}Pt_2Sn_{3.73}$
Formula mass	333.25	767.07	830.41	848.79
Crystal system	cubic	cubic	cubic	cubic
a (pm) single crystal	626.1(1)	1264.3(1)	1266.6(1)	1269.7(2)
a (pm) powder sample	626.0(1)	1264.4(2)	1266.6(2)	1270.2(4)
Volume (nm^3)	0.02453	0.20214	0.20320	0.20494
Space group	$F\bar{4}3m$	$Ia\bar{3}$	$Ia\bar{3}$	$Ia\bar{3}$
Pearson Symbol	c*F*16	c*I*128	c*I*128	c*I*128
Z	4	16	16	16
ρ_{calc} (gcm^{-3})	9.018	10.084	10.859	11.017
Crystal size (μm^3)	50 × 60 × 90	40 × 40 × 40	80 × 50 × 8	15 × 25 × 55
Transmission ratio (max/min)	4.04	1.65	3.22	2.92
λ (Mo-K_α) pm	71.073	71.073	71.073	71.073
μ (mm^{-1})	67.2	69.62	71.98	72.22
F(000)	545	5040	5466	5590
Detector distance (mm)	60	60	60	50
Exposure time (min)	35	8	12	20
ω range (°); increment (°)	0−180; 1.0	−	0−180; 1.0	−
range (°); increment (°)	360	2−200/1.2	360	0−180/1.5
Profile/pixel	−	9−21	−	9−25
Pixelsize (mm)	0.15	−	0.15	−
Profile parameters				
A, B,	15.0/6.0	−/−	15.8, 3.8	−/−
EMS	0.024	0.010	0.039	0.011
θ range (°)	5−33	3−28	3−32	3−30
Total data collected	822	7566	12098	10123
Range in *hkl*	±9, ±9, ±9	±16, ±16, ±16	±19, ±19, ±19	±17, ±17, ±17
Unique data	70	416	620	521
Observed data [$I > 2\sigma(I)$]	70	389	561	167
Refinement method	Full-matrix least-squares on F^2			
$R_{internal}$ / R_{sigma}	0.2439/0.0962	0.0521/0.0172	0.1114/0.0318	0.1140/0.0406
R indices [$I > 2\sigma(I)$]				
R_1, *wR*2	0.0461/0.0834	0.0166/0.0335	0.0411/0.1043	0.0321/0.0795
R (all data)				
R_1, *wR*2	0.0461/0.0834	0.0192/0.0340	0.0483/0.1094	0.1131/0.1130
Weight parameters *a*, *b*	0.0358/0.8761	0.0208/0	0.0394/80.625	0.0380/0
Goodness of fit (S_{obs})	1.191	1.001	1.098	0.770
No. of variables, restraints	7/0	23/0	25/0	24/0
Twin, *BASF*	−	−	−	0.487(7)
Extinction coefficient	0.0013(8)	0.000062(5)	0.00011(2)	0.00016(2)
Largest diff. peak and hole e·Å^{-3}	4.120/−2.965	1.002/−1.025	2.074/−1.925	1.593/−1.982

Table 2. Atomic coordinates and isotropic displacement parameters [pm^2] for $Li_{1.96(2)}PtSn_{1.04(2)}$, $Li_3Pt_2Sn_3$, $Li_{2.27(1)}Pt_2Sn_{3.73(1)}$ and $Li_{2.43(1)}Pt_2Sn_{3.57(1)}$; U_{eq} is defined as one third of the trace of the orthogonalized U_{ij} tensor

Atom	Occ.	Wyckoff position	x	y	z	U_{eq}/U_{iso}
			$Li_{1.96(2)}PtSn_{1.04(2)}$			
Li1	0.96(2)	4*b*	1/2	0	0	20(10)[a]
Li2	1	4*d*	3/4	3/4	3/4	71(95)
Pt	1	4*a*	0	0	0	23.4(6)
Sn1	1	4*c*	1/4	3/4	3/4	26(1)
Sn2	0.04(2)	4*b*	1/2	0	0	20(10)[a]
			$Li_3Pt_2Sn_3$			
Li1	1	16*c*	0.121(1)	x	x	25(5)
Li2	1	8*a*	0	0	0	31(8)
Li3	1	24*d*	1/4	0.253(2)	0	69(13)
Pt1	1	8*b*	1/4	1/4	1/4	8.3(1)
Pt2	1	24*d*	1/4	0.47895(3)	0	8.5(1)
Sn	1	48*e*	0.11611(3)	0.35634(4)	0.12176(3)	11.7(1)
			$Li_{2.27(1)}Pt_2Sn_{3.73(1)}$			
Li1	0.27(1)	16*c*	0.1241(1)	x	x	12.2(8)[a]
Li2	1	8*a*	0	0	0	22(21)
Li3	1	24*d*	1/4	0.251(4)	0	26(13)
Pt1	1	8*b*	1/4	1/4	1/4	8.6(4)
Pt2	1	24*d*	1/4	0.49513(8)	0	10.8(4)
Sn1	1	48*e*	0.1228(1)	0.3706(1)	0.1243(1)	16.9(4)
Sn2	0.73(1)	16*c*	0.1241(1)	x	x	12.2(8)[a]
			$Li_{2.43(1)}Pt_2Sn_{3.57(1)}$			
Li1	0.43(1)	16*c*	0.1246(2)	x	x	18.7(7)[a]
Li2	1	8*a*	0	0	0	2(7)
Li3	1	24*d*	1/4	0.2472(16)	0	12(7)
Pt1	1	8*b*	1/4	1/4	1/4	13.0(3)
Pt2	1	24*d*	1/4	0.49013(7)	0	17.3(3)
Sn1	1	48*e*	0.12086(7)	0.3663(1)	0.1230(1)	21.4(3)
Sn2	0.57(1)	16*c*	0.1246(2)	x	x	18.7(7)[a]

[a] The displacement parameters are constrained to be equal and the sum of Li1 and Sn2 are set to 100% occupancy.

Thus, the content of lithium can be increased further. This is done by substitution of tin at the tetrahedral sites by lithium atoms. Gradually the lithium content can be increased from $LiPtSn_2$ to $Li_3Pt_2Sn_3$, where 2/8 of the tin atoms are replaced. The general formula of the new ternary compound may be written as $Li_{octahedra}[Pt(Sn_{1.5+x}Li_{tetrahedra\ 0.5-x})]$ with $x = 0-0.5$ for the fluorite-type subcell i.e. $Li_2[Pt_2(Sn_{3+x}Li_{1-x})]$ with $x = 0-1$ for the superstructure.

Seven single crystals were refined and their lattice parameters found to correlate nicely with the amount of lithium on the tetrahedral sites (Figure 2). Decreasing the tin content lets the lattice parameter drop mainly because the smaller lithium atoms substitute the larger tin atoms (123 pm and 140 pm for lithium and tin, respectively).[19] Along with this substitution the intensities of the superstructure reflections increase in intensity to reach a maximum at the ideal composition for the superstructure of $Li[Pt(Sn_{1.5}Li_{0.5})]$ i.e. $Li_3Pt_2Sn_3$.

The following discussion reflects on the consequences of the ordered arrangement of lithium and tin for the near neighbour environment (Figure 3). The filling of octahedral sites by lithium in a fluorite-type subcell increases the coordination numbers (CN) of platinum and tin and lithium as well. CNs of 8, 9 and 10 are found for Pt1, Pt2 and Sn, respectively. The CNs for the lithium atoms are 14, 8 and 9 for Li1, Li2 and Li3, respectively. The high CN of Li1 can be explained as follows. The lithium atom Li1 replaces 2/8 of the tin positions of the subcell. This would lead to CN 8 i.e. four tetrahedrally oriented platinum atoms and four lithium atoms on octahedral sites. In the superstructure, however, shorter Pt−Sn distances of 270−276 pm (Table 4) occur as compared to those in binary $PtSn_2$ (278 pm). This shrinkage allows extra atoms to be in contact with the Li1 atoms. Due to the additional lithium on octahedral voids of the *fcc* arrangement of the platinum atoms and the order of tin and lithium on tetrahedral voids, all near-neighbour environments are basically strongly distorted cubes with six additional atoms on faces and edges increasing the CN.

In Li_2PtSn the lithium content seems to reach the maximum possible, where 4/8 of the tin positions are occupied by lithium atoms. The lattice parameter fits well in the *a* vs. *portion Li* plot of Figure 2, indicating again that the drop of the lattice parameter is due to the size difference of Li/Sn of 123/140 pm (Pauling's radii).

Li_2PtSn constitutes the second ordered superstructure in the large range of fluorite-related structures in the Li-Pt-Sn system. It derives from the binary BiF_3 (a filled fluorite type) where bismuth forms a *fcc* arrangement and the two different fluoride sites occupy the tetrahedral and octahedral voids on 4*b* and 8*c* in $Fm\bar{3}m$, respectively (Figure 1). As compared to CaF_2, the Li2 atoms replace 4/8 of the fluoride positions in an ordered manner. This leads to a reduction in symmetry. The structure becomes non-centro-

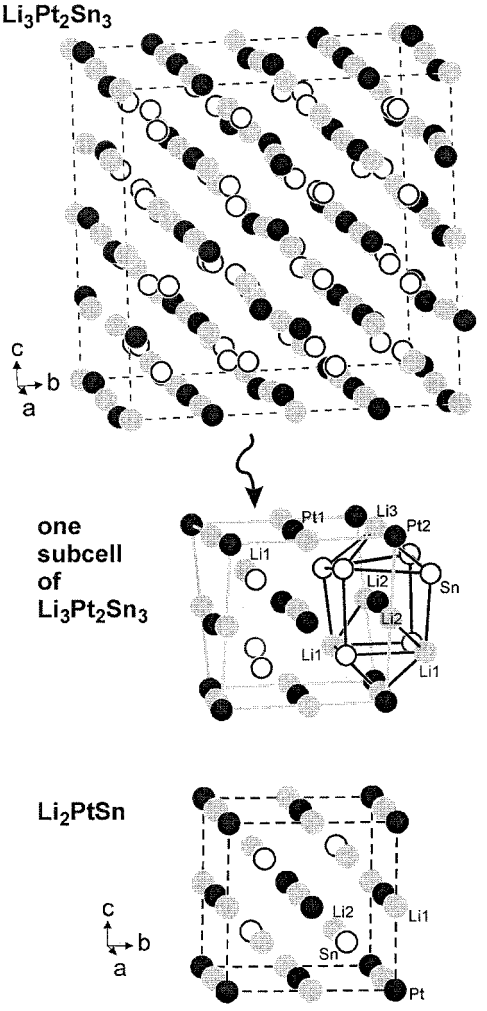

Figure 1. The crystal structures of $Li_3Pt_2Sn_3$ and Li_2PtSn; the lithium, platinum and tin atoms are drawn as grey, filled and open circles, respectively; at the top the $2 \times 2 \times 2$ supercell of $Li_3Pt_2Sn_3$ is shown; one subcell of $Li_3Pt_2Sn_3$ is outlined in the middle; note that in the solid solution $Li_{3-x}Pt_2Sn_{3+x}$ the Li1 position is additionally occupied by tin atoms; the similarity of the subcell with the ternary ordered BiF_3-type Li_2PtSn is emphasised below

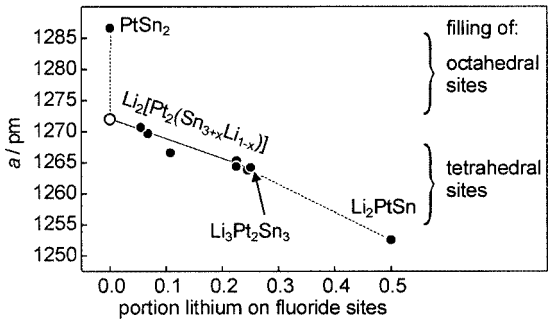

Figure 2. Course of the cubic lattice parameter of the solid solution $Li_{3-x}Pt_2Sn_{3+x}$, $PtSn_2$ and Li_2PtSn; for the latter two compounds the lattice parameters are doubled for comparison; the open circle marks the composition with the lowest lithium content possible of the solid solution where no tin/lithium mixing on the tetrahedral sites occur; the different filling mechanisms by lithium atoms are indicated on the right hand side of the drawing; filling of tetrahedral sites corresponds to a replacement of tin atoms

symmetric and it crystallises in the space group $F\bar{4}3m$, a *translationengleiche* subgroup of index 2 of $Fm\bar{3}m$ (Figure 4, upper right-hand side). The indide $LiPdIn_2$[12] actually crystallises in $Fm\bar{3}m$ representing a ternary ordered version of BiF_3. In Figure 4 the substitution of tin by lithium can be seen by the splitting of the 8*c* site of $Fm\bar{3}m$ into two fourfold sites 4*c* and 4*d* of $F\bar{4}3m$.

There is no direct group-subgroup relation between $F\bar{4}3m$ and $Ia\bar{3}$ because $F\bar{4}3m$ is non-centrosymmetric and one cannot gain symmetry. In addition, following the Bärnighausen formalism strictly,[20,21] filled structures are also excluded from a symmetry tree. Li_2PtSn and $Li_3Pt_2Sn_3$ have the same aristotype (BiF_3), but both are situated on different branches.

BiF_3 is a filled CaF_2 type. For clarity the empty octahedral sites are left out on the CaF_2 branch (left hand side of Figure 4). Within the CaF_2 branch it is improbable that the interim AX_2 phases exist, and in actual fact they do not have to. So far no intermetallics with the symmetry $Pm\bar{3}m$ or $Pm\bar{3}$ and the atomic positions given in Figure 4 are known. One might speculate that a ternary stannide with two different transition metals on the sites 1*a* (A1) and 3*c* (A′2) of $Pm\bar{3}m$ exists. The necessary distortions are already

Table 3. Lattice parameters of $PtSn_2$[26] and the various ternary lithium-platinum stannides Li_2PtSn and $Li_{3-x}Pt_2Sn_{3+x}$

Compound	*Octahedra*[Pt(*Tetrahedra*)]	*a*/pm	Portion of tetrahedral Li
$PtSn_2$	[Pt(Sn_2)]	1286.62	0
Li_2PtSn	Li[Pt(SnLi)]	1252.2(2)	0.5
$Li_3Pt_2Sn_3$	Li_2[Pt_2(Sn_3Li)]	1264.2(1)	0.25
$Li_{2.98}Pt_2Sn_{3.02}$	Li_2[Pt_2($Sn_{3.02}Li_{0.98}$)]	1263.89(8)	0.245
$Li_{2.9}Pt_2Sn_{3.1}$	Li_2[Pt_2($Sn_{3.1}Li_{0.9}$)]	1265.3(2)	0.225
$Li_{2.9}Pt_2Sn_{3.1}$	Li_2[Pt_2($Sn_{3.1}Li_{0.9}$)]	1264.94(9)	0.225
$Li_{2.43}Pt_2Sn_{3.57}$	Li_2[Pt_2($Sn_{3.57}Li_{0.43}$)]	1266.6(1)	0.1075
$Li_{2.27}Pt_2Sn_{3.73}$	Li_2[Pt_2($Sn_{3.73}Li_{0.27}$)]	1269.7(2)	0.0675
$Li_{2.22}Pt_2Sn_{3.78}$	Li_2[Pt_2($Sn_{3.78}Li_{0.22}$)]	1270.7(2)	0.055

Table 4. Interatomic distances [pm], calculated with the lattice parameters taken from the single crystal diffractometer measurements of Li_2PtSn and $Li_3Pt_2Sn_3$; all distances of the first coordination spheres are listed; standard deviations are all equal or less than 1 pm

			Li_2PtSn				
Li1	4	Li2	271.1				
	4	Sn	271.1				
	6	Pt	313.1				
Li2	4	Li1	271.1				
	4	Pt	271.1				
	6	Sn	313.1				
Pt	4	Li2	271.1				
	4	Sn	271.1				
	6	Li1	313.1				
Sn	4	Li1	271.1				
	4	Pt	271.1				
	6	Li2	313.1				
			$Li_3Pt_2Sn_3$				
Li1	1	Li2	265.4	Pt2	2	Sn	268.7
	3	Li3	278.9		2	Sn	271.5
	1	Pt1	282.1		2	Sn	276.4
	3	Pt2	287.0		1	Li3	285.7
	3	Sn	297.4		2	Li1	287.0
	3	Sn	301.4		2	Li2	317.2
Li2	2	Li1	265.4		2	Li3	317.2
	6	Sn	279.7		1	Li3	346.5
	6	Pt2	317.2	Sn	1	Li3	259.1
Li3	2	Sn	259.1		1	Li3	263.5
	2	Sn	263.5		1	Pt2	268.7
	2	Li1	278.9		1	Pt1	270.2
	1	Pt2	285.7		1	Pt2	271.5
	2	Sn	294.4		1	Pt2	276.4
	2	Pt1	316.1		1	Li2	279.7
	2	Pt2	317.2		1	Li3	294.4
	1	Pt2	346.5		1	Li1	297.4
Pt1	6	Sn	270.2		1	Li1	301.4
	2	Li1	282.1		2	Sn	334.4
	6	Li3	316.1		2	Sn	337.4

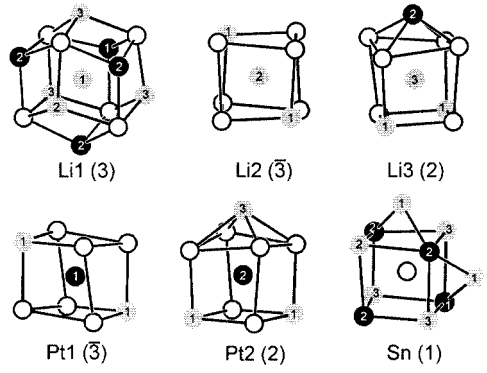

Figure 3. Near neighbour environment in the structure of $Li_3Pt_2Sn_3$; the lithium, platinum and tin atoms are drawn as grey, filled and open circles, respectively; the numbers correspond to the atom designations; the site symmetries are given in parentheses

taken care of by the extra parameter x of the X (Sn) position in 8*g*. Nevertheless, at this point the two different platinum sites of $Li_3Pt_2Sn_3$ already come into play. Both have different average distances to lithium and tin (Table 4).

The gain of the next *klassengleiche* symmetry reduction of index 4 (doubling in all three directions) is the most important one. It allows ordering of the tin and lithium atoms in the ratio 3:1. This was the key in solving the superstructure. It also means that this reduction is a one-way direction. The tin/lithium ratio on the tetrahedral sites is now fixed to 3:1 and cannot be changed unless further symmetry reductions occur. The consequence of this is that there is no solid solution between $Li_3Pt_2Sn_3$ and Li_2PtSn, because Li_2PtSn crystallises with a higher symmetry. Nevertheless, as Figure 2 suggests, the different volume increments of tin/lithium determine the course of the lattice parameters of $Li_3Pt_2Sn_3$ and Li_2PtSn.

To sum up, the crystal chemical relation between the different ternary lithium stannides is nicely depicted by the symmetry tree given in Figure 4. There are different mechanisms of establishing a certain lithium/tin ratio by filling octahedral and tetrahedral voids with lithium and lithium/tin mixtures, respectively, in the *fcc* arrangement of platinum.

Experimental Section

General: Starting materials for the preparation of the lithium-platinum-stannides were lithium rods (Merck, >99%), platinum powder (Degussa-Hüls, 200 mesh, >99.9%) and a tin bar (Heraeus, 99.9%). The lithium rods were cut into smaller pieces under dry paraffin oil and subsequently washed with *n*-hexane. The paraffin oil and *n*-hexane were previously dried over sodium wire. The lithium pieces were kept in Schlenk tubes under argon prior to the reactions. Argon was purified over titanium sponge (900 K), silica gel and molecular sieves.

The lithium pieces were mixed with cold-pressed pellets of platinum powder and pieces of the tin bar in the respective atomic ratios and sealed in tantalum ampoules under an argon pressure of about 800 mbar in an arc-melting apparatus.[22] The tantalum tubes were then sealed in evacuated silica tubes to prevent oxidation, rapidly heated at 1070 K and held at this temperature for between three hours and one day. The temperature was then lowered to 720 K or 820 K within four days followed by slow cooling to room temperature by switching off the furnace. The samples could be readily separated from the tubes. No reaction with the container material was observed. The light grey, polycrystalline compounds are stable in air over several weeks. Single crystals exhibit a metallic lustre.

X-ray investigations

The samples were characterised from Guinier patterns or powder diffractograms (Stoe StadiP) using Cu-$K\alpha_1$ radiation and silicon (a = 543.07 pm) as external standard or α-quartz (a = 491.30 pm, c = 540.46 pm) as internal standard. The cubic lattice parameters (Table 1) were obtained from least-squares fits of the powder data. The correct indexing of the patterns was facilitated by intensity calculations[23] taking the atomic positions from the structure refinements. The lattice parameters determined from the powders and the single crystals agreed well.

Several silvery, irregularly shaped single crystals of the solid solution were isolated from the annealed samples by mechanical fragmentation. They were examined on a Buerger precession camera equipped with an image plate system (Fujifilm BAS-2500 and -1800) in order to establish suitability for intensity data collection.

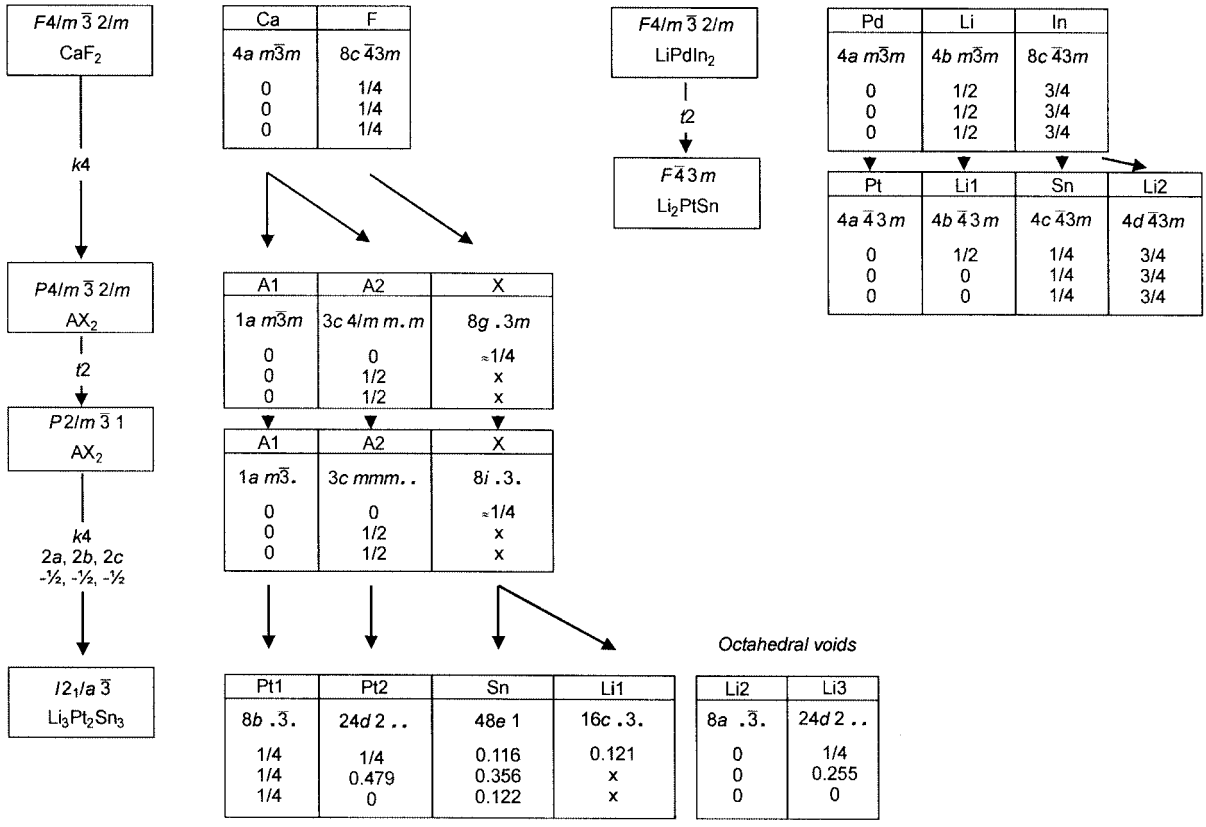

Figure 4. Group-subgroup relation in the Bärnighausen formalism[20,21] for the structures of CaF_2, $Li_3Pt_2Sn_3$, $LiPdIn_2$ and Li_2PtSn; the indices of the *klassengleiche* (k) and *translationengleiche* (t) transitions, the unit cell transformations with origin shifts and the evolution of the atomic parameters are given; the octahedral voids in CaF_2 and the interim structures are left out for clarity; $LiPdIn_2$ constitutes a ternary ordered version of BiF_3, which is a filled fluorite type

Single-crystal intensity data were collected at room temperature by use of a four-circle diffractometer (CAD4) with graphite-monochromated Mo-K_α radiation (71.073 pm) and a scintillation counter with pulse height discrimination. The scans were performed in the $\omega/2\theta$ mode. Empirical absorption corrections were applied on the basis of Ψ-scan data. Some data sets were collected on a Stoe IPDS-I and IPDS-II diffractometer with graphite monochromated Mo-K_α radiation. All relevant crystallographic data and experimental details for the data collections are listed in Table I.

Structure Refinements

The starting atomic parameters for the platinum and tin atoms were deduced from automatic interpretations of direct methods with SHELXS-97.[24] The lithium positions were determined from subsequent difference Fourier analyses. The structures were then refined using SHELXL-97 (full-matrix least-squares on F_o^2)[25] with anisotropic atomic displacement parameters for tin and platinum while isotropic refinement was carried out for the lithium atoms.

Refinement of Li_2PtSn

The determination of the space group for Li_2PtSn was carried out as follows. Reciprocal space revealed only the extinction conditions for a cubic face centred lattice. No extra extinctions were observed. Therefore, $Fm\bar{3}m$ was chosen as the highest symmetry space group possible. The refinement went smoothly to low R values ($R1$ = 0.032) assuming a fluorite-type structure with platinum occupying the calcium sites and a 1:1 mixture of tin and lithium on the fluoride sites. The drawback of this refinement, of course, is the mixed Sn/Li occupancy and that the occupation of additional octahedral sites by lithium could not be detected in a difference Fourier synthesis. However, the subgroup $F\bar{4}3m$ of $Fm\bar{3}m$ allows ordering of the tin/lithium atoms on the fluoride positions. This refinement yielded a reasonable R value, but not as low as the refinement in $Fm\bar{3}m$. In addition, a final difference Fourier synthesis revealed the occupancy of the octahedral voids leading to the composition Li_2PtSn. Careful inspection of the displacement parameters and the difference Fourier synthesis suggested a slight mixing of tin and lithium on the octahedral sites resulting in the composition $Li_{1.96(2)}PtSn_{1.04(2)}$. Despite the fact that the final R value is actually higher than the refinement in $Fm\bar{3}m$, the structure is correctly described in $F\bar{4}3m$. This is also undermined by the refined Flack parameter of 0.01(6), indicating the correct absolute orientation. In addition, the Flack parameter is expected to be 0.5 in the case where $Fm\bar{3}m$ is the correct space group.

$Li_{3-x}Pt_2Sn_{3+x}$: Refinement of $Li_3Pt_2Sn_3$, $Li_{2.27}Pt_2Sn_{3.73}$ and $Li_{2.43}Pt_2Sn_{3.57}$

The strongly dominating subcell of $Li_3Pt_2Sn_3$ with $a' = 1/2a$ belongs to a fluorite type as does Li_2PtSn. Indeed, the atomic positions of the binary fluorite phase $PtSn_2$ served as a starting point. Both lithium and tin occupy the fluoride positions with a refined ratio of approximately 3:1. The difference Fourier synthesis indicated additional occupation of octahedral voids by lithium, but in the subcell those positions were not refinable. This is due to the high cubic symmetry and parameter correlations. However, these correlations were nicely resolved in the superstructure.

All three lattice parameters are doubled in the superstructure. This means in terms of symmetry reduction that one has to decentre the *F*-lattice first to get a primitive lattice and subsequently double a', b' and c'. The extinction conditions of the many weak superstructure reflections were compatible with a body centred lattice and showed the presence of an *a*-glide plane. Only one cubic space group was possible, $Ia\bar{3}$, in which the superstructure was refined successfully. Also, $Ia\bar{3}$ allows ordering of the lithium and tin atoms on the fluoride positions of the subcell in the ratio 1:3.

The ternary stannide follows the general formula $Li_{3-x}Pt_2Sn_{3+x}$. To cover the whole range of homogeneity a total of seven single crystals were refined for which x varied between $x = 0$ and $x = 0.78$. The crystals originated from samples with four different starting compositions, Li:Pt:Sn = 1:1:4, 1:1:2, 1:1:1 and 3:2:3.

The lattice parameters were refined from powder data as well and matched those obtained for the single crystal. We did not obtain pure samples in all cases as the starting compositions suggest. Therefore the lattice parameters obtained from the single crystal were taken to calculate atomic distances for the various structures refined. Apparently inhomogeneity with respect to the composition $Li_{3-x}Pt_2Sn_{3+x}$ could not be avoided as additional shoulders next to the strongest reflections suggested. Nevertheless, the lattice parameters in a single powder sample were within a narrow range and smaller than the variation of the lattice parameters over the whole range of homogeneity.

Two of the seven data sets were collected from crystals that showed twinning by merohedry. This twinning is suggested by the *translationengleiche* symmetry reduction t2 i.e. losing the high Laue symmetry. Consequently the twin matrix is 0 1 0, 1 0 0, 0 0 −1. Only three refinements are reported here, corresponding to the compositions, $Li_3Pt_2Sn_3$, $Li_{2.27}Pt_2Sn_{3.73}$ and $Li_{2.43}Pt_2Sn_{3.57}$. The other four data sets were refined to similar results, but give only redundant information.

The course of the structure refinement will be discussed for $Li_3Pt_2Sn_3$ as an example. The platinum and tin positions were calculated in going from the subcell positions to the supercell positions according to the symmetry reductions given in a Bärnighausen scheme[20,21] (Figure 4). The three lithium positions were clearly revealed by a difference Fourier synthesis. For the ideal composition $Li_3Pt_2Sn_3$ no remaining electron density on the lithium sites was observed and the displacement parameters of the lithium atoms behaved well. This occurred quite differently within the solid solution. Here, large difference Fourier peaks on the lithium site 16*c* could be observed. The only explanation, supported by the varying lattice parameters, was a mixed occupancy by tin atoms. The 16*c* site was occupied by Li1 and additional Sn2 atoms assuming that the sum was 100% (Table 2). The atomic positions and displacement parameters were constrained to be equal. Thus, the refinement of the lithium content was riding on the larger scattering power of tin on the site 16*c*, even though increasing tin/lithium mixing lets the intensity of the superstructure reflections gradually diminish.

Final difference Fourier syntheses revealed no significant residual peaks (see Table 1). The positional parameters of the refinements are listed in Table 2. Table 3 contains additional information regarding the range of homogeneity. In Table 4 the interatomic distances of the ideal structures are listed. Listings of the observed and calculated structure factors are available.
Further details of the crystal-structure investigation(s) may be obtained from the Fachinformationszentrum Karlsruhe, 76344 Eggenstein-Leopoldshafen, Germany, on quoting the depository number(s) CSD-413190 (Li_2PtSn), -413187 ($Li_3Pt_2Sn_3$), -413188 ($Li_{2.27}Pt_2Sn_{3.73}$) and -413189 ($Li_{2.43}Pt_2Sn_{3.57}$).

Acknowledgments

We thank the Degussa-Hüls AG for a generous gift of platinum powder. This work was financially supported by the Fonds der Chemischen Industrie and by the Deutsche Forschungsgemeinschaft through SFB 458 Ionenbewegung in Materialien mit ungeordneten Strukturen.

[1] F. Hund, R. Fricke, *Z. Anorg. Allg. Chem.* **1949**, *258*, 198.
[2] P. Villars, L. D. Calvert, *Pearson's Handbook of Crystallographic Data for Intermetallic Phases*, second ed. and desk ed., ASM International, Materials Park, OH, **1991** and **1997**.
[3] H.-U. Schuster, D. Thiedemann, H. Schönemann, *Z. Anorg. Allg. Chem.* **1969**, *370*, 160.
[4] A. Czybulka, D. Last, H.-U. Schuster, *Metall−Metall-Wechselwirkungen in Zintl-Verbindungen und intermetallischen Phasen verwandter Struktur*, in B. Krebs, *Unkonventionelle Wechselwirkungen in der Chemie metallischer Elemente*, VCH, chapter 17, **1992**.
[5] H. Pauly, A. Weiss, H. Witte, *Z. Metallkd.* **1968**, *59*, 47.
[6] A. Czybulka, A. Petersen, H.-U. Schuster, *J. Less-Common Met.* **1990**, *161*, 303.
[7] J. Drews, U. Eberz, H.-U. Schuster, *J. Less-Common Met.* **1986**, *116*, 271.
[8] M. M. Thackeray, K. D. Kepler, J. T. Vaughey, Patent No. WO 2000003443, Application No. WO 1999-US12868.
[9] Zh. Wu, R.-D. Hoffmann, D. Johrendt, B. D. Mosel, H. Eckert, R. Pöttgen, *J. Mater. Chem.* in press.
[10] L. Drews-Nicolai, G. Hohlneicher, *J. Alloys Compd.* **2001**, *316*, 1.
[11] L. Drews-Nicolai, G. Hohlneicher, U. Hoppe, W. Jung, *Z. Anorg. Allg. Chem.* **2001**, *627*, 1157.
[12] R. Pöttgen, Zh. Wu, R.-D. Hoffmann, G. Kotzyba, H. Trill, J. Senker, D. Johrendt, B. D. Mosel, H. Eckert, *Heteroatom Chem.* **2002**, *6*, 506.
[13] Zh. Wu, H. Eckert, J. Senker, D. Johrendt, G. Kotzyba, B. D. Mosel, H. Trill, R.-D. Hoffmann, R. Pöttgen, *J. Phys. Chem. B* **2003**, *107*, 1943.
[14] Zh. Wu, H. Eckert, B. D. Mosel, R. Pöttgen, *Z. Naturforsch., Teil B* **2003**, *58*, 501.
[15] H. J. Wallbaum, *Z. Metallkd.* **1943**, *35*, 200.
[16] C. J. Kistrup, H. U. Schuster, *Z. Anorg. Allg. Chem.* **1974**, *410*, 113.
[17] C. J. Kistrup, H. U. Schuster, *Z. Naturforsch., Teil B* **1972**, *27*, 324.
[18] J. Donohue, *The Structures of the Elements*, Wiley, New York, **1974**.
[19] J. Emsley, *The Elements*, Oxford University Press, 3rd edn, **1999**.
[20] H. Bärnighausen, *Commun. Math. Chem.* **1980**, *9*, 139.
[21] H. Bärnighausen, U. Müller, *Symmetriebeziehungen zwischen den Raumgruppen als Hilfsmittel zur straffen Darstellung von Strukturzusammenhängen in der Kristallchemie*, University of Karlsruhe and University/GH Kassel, Germany, **1996**.
[22] R. Pöttgen, Th. Gulden, A. Simon, *GIT-Laborfachzeitschrift* **1999**, *43*, 133.
[23] K. Yvon, W. Jeitschko, E. Parthé, *J. Appl. Crystallogr.* **1977**, *10*, 73.
[24] G. M. Sheldrick, SHELXS-97, *Program for the Solution of Crystal Structures*, University of Göttingen, Germany, **1997**.
[25] G. M. Sheldrick, SHELXL-97, *Program for Crystal Structure Refinement*, University of Göttingen, Germany, **1997**.
[26] J. S. Charlton, M. Cordey-Hayes, I. R. Harris, *J. Less-Common Metals* **1970**, *20*, 105.

Received May 27, 2003

